

# The glitches of the Anomalous X-ray Pulsar 1RXS J170849.0–400910

S. Dall'Osso<sup>1,2</sup> G. L. Israel<sup>2,3</sup>, L. Stella<sup>2,3</sup>, A. Possenti<sup>4,5</sup>, E. Perozzi<sup>6</sup>

## ABSTRACT

We report on a timing analysis of archival observations of the Anomalous X-ray Pulsar 1RXS J170849.0–400910 made with the RXTE Proportional Counter Array. We detect a new large glitch ( $\Delta\nu/\nu \simeq 3 \times 10^{-6}$ ) which occurred between 2001 March 27 and 2001 May 6, with an associated large increase in the spin-down rate ( $\Delta\dot{\nu}/\dot{\nu} \simeq 0.3$ ). The short time (1.5 yrs) elapsed from the previously detected glitch and the large amplitude of the new spin-up place this source among the most frequent glitchers, with large average glitch amplitudes, similar to those of the Vela pulsar. The source shows different recoveries after the glitches: in the first one it is well described by a long term linear trend similar to those seen in Vela-like glitches; in the second case the recovery is considerably faster and is better described by an exponential plus a fractional change in the long-term spin-down rate of the order of 1%. No recovery of the latter is detected but additional observations are necessary to confirm this result. We find minor but significant changes in the average pulse profile after both glitches. No bursts were detected in any lightcurve, but our search was limited in sensitivity with respect to short ( $t < 60$  ms) bursts. Observed glitch properties are compared to those of radio pulsar glitches; current models are discussed in light of our results. It appears that glitches may represent yet another peculiarity of AXPs. Starquake-based models appear to be preferred on qualitative grounds. Alternative models can be applied to individual glitches but fail in explaining both. Thus the two events may as well arise from two different mechanisms.

---

<sup>1</sup>Università degli Studi di Roma “La Sapienza”, P.zza Aldo Moro 5, I-00195 Roma, Italy

<sup>2</sup>INAF - Osservatorio Astronomico di Roma, V. Frascati 33, I-00040 Monteporzio Catone (Roma), Italy;  
dallosso, gianluca and stella@mporzio.astro.it

<sup>3</sup>Affiliated to the International Center for Relativistic Astrophysics

<sup>4</sup>INAF - Osservatorio Astronomico di Bologna, via Ranzani 1, 40127 Bologna, Italy

<sup>5</sup>INAF - Osservatorio Astronomico di Cagliari, Loc. Poggio dei Pini, Strada 54, 09012 Capoterra (CA),  
Italy; possenti@ca.astro.it

<sup>6</sup>Telespazio, Via Tiburtina 965, 00156 Roma, Italy; Ettore\_Perozzi@telespazio.it

*Subject headings:* stars: neutron – pulsars: general – X-rays: stars – X-rays: individual (1RXS J170849.0–400910)

## 1. Introduction

AXPs are a small class of X-ray pulsars whose luminosity, though somewhat lower ( $10^{34}$ – $10^{36}$  erg s $^{-1}$ ) and much softer than that of standard X-ray pulsars, largely exceeds their rotational energy losses ( $\sim 10^{32}$ – $10^{33}$  erg s $^{-1}$ ). The association with systems accreting matter at low level (Mereghetti & Stella 1995, Van Paradijs et al. 1995, Chatterjee et al. 2000, Alpar 2001) is made problematic by some of the observational properties that ultimately characterize AXPs as a distinct class. These are their fairly steady spin-down, clustering in a narrow range of spin periods (6–12 sec) and absence of conspicuous counterparts at other wavelengths (Mereghetti & Stella 1995, Mereghetti et al. 2002). For three of these objects very weak infrared counterparts have so far been identified (Hulleman et al. 2001, Wang & Chakrabarty 2002, Israel et al. 2002, Israel et al. 2003). In one case an optical counterpart, with pulsations at the X-ray period, was found (Kern & Martin 2002). Though faint, these optical/IR counterparts are far too bright with respect to the extrapolation of a blackbody-like spectrum matching the X-ray emission. The origin of the optical/IR emission of AXPs remains to be understood (Israel et al. 2003).

Furthermore, both enhancements of the noise level and short-duration bursts in the X-ray emission of some sources have been found after years of monitoring (Kaspi et al. 2001, Gavriil and Kaspi 2002a) and evidence for a spin-up event consistent with a radio pulsar-like glitch has been found in RXS J170849.0–400910 (Kaspi et al. 2000, Gavriil and Kaspi 2002b). This lent additional support to the idea that AXPs may be magnetars, isolated neutron stars endowed with a huge magnetic field ( $B > 3 \times 10^{14}$  G) whose energy provides the reservoir to power the X-ray luminosity. This would link them to SGRs, a small class of bursting X-ray sources sharing with AXPs a comparable quiescent X-ray luminosity as well as similar periods and spin-down rates. For SGRs, several independent arguments hint to the presence of extremely high magnetic fields (Thompson & Duncan 1995). Very recently this picture has received compelling evidence by the detection of an SGR-like X-ray outburst in 1E 2259+586 (Kaspi et al. 2003). Associated with the outburst a glitch was also detected, with a large amplitude in the rotation rate ( $\Delta\nu/\nu \sim 4 \times 10^{-6}$ ) and extreme amplitude in the spin-down rate ( $\Delta\dot{\nu}/\dot{\nu} \sim 1$ ). Remarkably, no such direct connection has ever been observed, even in the case of SGR bursts (Woods et al. 2003, 2002), apart indirect evidence in one case (Woods et al. 1999).

Given the previous detection of a glitch in RXS J170849.0–400910, we decided to analyse

timing data following the glitch since the study of the long-term recovery of the source, including the possible occurrence of new glitches within a couple of years, would allow a closer comparison with the properties of known glitching radio pulsars. Indeed, glitches in ‘adolescent’ radio pulsars ( $t_s \sim 10^3 \div 10^5$  yrs) repeat at intervals of a few years or less, while many of the youngest and oldest radio pulsars have much sparser glitches, if at all. In the magnetar model the influence of the magnetic field on the structure and dynamical evolution of a neutron star is expected to produce features that may be peculiar to AXPs and can be identified by precision timing.

## 2. Data selection

We analyzed data from archival observations of RXS J170849.0–400910 carried out with the RXTE Proportional Counter Array (PCA). The total data set spans more than 4 years, between 1998 January 13 and 2002 May 29.

The PCA is made up of five PCUs each split in two, an upper propane layer and the main Xenon volume through which run 3 different Xenon layers. We analyzed data in the GoodXenonwithPropane configuration, in which single events, each coming from one of the 3 Xenon layers of one of the PCUs, are recorded in sequence at  $1\mu\text{s}$  time resolution. Events are analyzed and recorded by two independent Event Analyzers (EAs) at the same time.

Following Kaspi et al. (2000), in order to maximize the sensitivity, the analysis was restricted to unrejected events in the top Xenon layer of each PCU and only soft photons were selected for extracting lightcurves, namely those collected in channels 6–14 (corresponding to the range  $\sim 2.5 - 6\text{keV}$ ).

Data from the two EAs were merged into a single lightcurve using the standard RXTE software and then rebinned at 62.5 ms resolution. Standard reduction to barycentric dynamical time (TDB) was then applied, using the (10'' accurate) source position given by Israel et al. (1999).

## 3. Data Analysis

A phase-coherent timing analysis was carried out using a phase-fitting technique, an iterative procedure allowing the determination of the frequency of a coherent signal *at a given epoch*, with a precision that increases as more observations are included in the analysis.

The signal from the source is assumed to be periodic

$$\phi(t) = \phi_0 + \int_{t_0}^t \omega(t') dt' \quad (1)$$

The steady variation of the period is parametrized by a series of time derivatives, truncated at the highest term which appears statistically significant.

After integration equation (1) reads:

$$\phi(t) = \phi_0 + \omega_0(t - t_0) + \frac{1}{2}\dot{\omega}_0(t - t_0)^2 + \frac{1}{6}\ddot{\omega}_0(t - t_0)^3 + \dots \quad (2)$$

where the  $\dots$  include all the terms in the series resulting from derivatives of  $\omega$  of order higher than the second.

A first guess period ( $P_0$ ) was determined through an epoch folding search of the lightcurve of an observation chosen as the starting point. Its epoch was adopted as the reference with respect to which all the following phases were calculated.

A template pulse-profile was then determined by folding this lightcurve at the period  $P_0$  and fitting the resulting binned pulse-profile with a template function of the form:

$$\psi(t) = \sum_{i=1}^n A_i \sin[i\omega_0(t - \psi_i)] \quad (3)$$

truncating the series at the highest armonic that was statistically significant after performing an F-test at the 99 % ( $2.7\sigma$ ) level.

The lightcurve was then divided in 4 intervals and each of them folded at the same  $P_0$ . The 4 resulting binned pulse-profiles were fit by the template function, with  $A_1$  and  $\psi_1$  as free parameters while keeping frozen the harmonics amplitude ratios ( $A_i/A_1$ ) and phase differences  $\psi_i - \psi_1$ . This is equivalent to assuming that the shape of the average pulse profile does not change. We checked this by verifying that the  $\chi^2$ 's were distributed around the expected value  $\langle \chi^2 \rangle = \nu$  with a dispersion comparable to  $\sigma_{\chi^2} = \sqrt{2\nu}$  with  $\nu$  the degrees of freedom of the model.

The values of  $\psi_1$  for the 4 intervals were then plotted versus the epochs and fitted by a function of the form (2), truncating that series at the last coefficient which was found to be statistically significant through an F-test at the 99% level. A 99% confidence interval for the value of the first parameter consistent with zero was also determined.

Phase-fitting applied to the four phases provides a correction to the guess period  $P_0$ , resulting in a better estimate of the period – call it  $P'$  – with a smaller uncertainty. The

lightcurve was folded again using  $P'$ , in order to have a more accurate template function.

Then we evaluated the maximum time interval  $\Delta t$  over which extrapolated phases remained coherent without any cycle ambiguity. Typically  $\Delta t \sim 8$  hrs when  $P$  is determined with a single observation whose duration is  $\sim 3$  ks. The observation selected as the starting point of our phase coherent analysis had a separation from the closest observation smaller than  $\Delta t$ .

Phase-coherence could then be maintained over the  $\sim 4$  days separating the first three observations. The addition of the third observation yielded as small an uncertainty on  $P$  ( $\sim$  some  $\mu$ s) that  $\Delta t \sim 40 \div 50$  days, enough to connect all the following observations, typically spaced by  $\sim 30$  days. Of course, the addition of more observations further decreases the uncertainties on  $P$ .

The fit to the fourth observation, more than 30 days apart from the first one, required the inclusion of a significant quadratic term ( $\dot{P}$ ) in Eq. (2).

From this point onwards the phase-coherent analysis was further extended by using the  $\dot{P}$  derived from the fits together with  $P$ , readjusting the values of both parameters at each step, checking for consistency with previous error intervals and readjusting the template function, that was always obtained after folding at the best  $P$  and  $\dot{P}$  all the lightcurves that had been connected with a single solution of equation (2).

By this procedure we analyzed all observations since January 13 1998 (MJD 50825). We detected the glitch already reported by Kaspi et al. (2000) between 1999 September 25 and 1999 October 21, as our timing solution failed to match the observed phases later than September 25 even with the addition of higher orders in the polynomial expansion of Eq. 2. The spin parameters previous and after the glitch and the inferred glitch parameters are reported in Tab. 1. We note that our results are in agreement with those of Kaspi et al. (2000) and Gavriil & Kaspi (2002b).

Time residuals after subtraction of our pre-glitch model are shown in Fig.1.

#### 4. New Data and Results

The set of new data started with 4 closely spaced observations , one made on 2001 May 6, two on May 11 and one on May 12 (MJD 52035, 52040 and 52041, respectively).

Fitting these observations with post-glitch N.1 model proved impossible: this is apparent in Fig.2, where the timing residuals after subtraction of the model for recovery from

glitch N.1 are shown and the sudden change in the star spin is clearly seen.

This feature is qualitatively similar to the 1999 glitch (see Kaspi et al. 2000), suggesting that another glitch may have happened between March 27 and May 6, 2001.

We then repeated the phase-fitting on the series of data from 2001 May 6 to 2002 May 29, taking as the reference epoch the middle point between the second May 11 and the May 12 observations. The latter had a longer duration ( $\sim 2.5$  ks) so we chose it as the starting point of a new phase coherent solution, in order to get as small an uncertainty on  $P_0$  as possible.

The separation between these two observations was too long ( $\sim 18$  hrs) for coherence to be maintained and there was an ambiguity of 1 cycle in the phases of the second observation due to a  $\sim 3$  ms uncertainty on  $P_0$  determined from the first one only. A coherent solution connecting the four observations between May 6 and May 12 could be found only assuming that a whole cycle had been missed from the first to the second one using that value of  $P_0$ . With this assumption the fit to the 4 observations was obtained with no significant period derivative.

The new  $P$  was  $\sim 20\mu\text{s}$  shorter than expected from extrapolation of the pre-glitch model and, when a fifth observation was added, a  $\dot{P}$  term was highly significant with a value greater than that measured before May 6. This is consistent with the positive  $\Delta\dot{P}$  expected from a glitch.

The parameters of the best-fit polynomial solution, up to the fourth frequency derivative, connecting all observations from 2001 May 6 to 2002 May 29 (MJD 52423) are reported in Tab.2 and residuals with respect to it are shown at the right of the vertical line in Fig.3.

We note, however, that the period evolution can be interpreted in a different way. Post-glitch recoveries of radio pulsars are usually described in terms of two different components with a long-term, approximately linear recovery of  $\dot{\nu}$  superposed to an initial, short-term exponential that, in some cases, has been resolved in the sum of a few exponentials with different timescales. The recovery fraction is usually defined as  $Q = \delta\nu_{exp}/(\delta\nu_{exp} + \Delta\nu_l)$  (Eq.4 below).

Thus, given the relatively fast recovery after glitch N.2 and the higher order polynomial coefficients required, we also tried fitting the phases following this glitch with the sum of an exponential and a linear trend. The same procedure was applied for consistency to the recovery from glitch N.1 as well. To this aim, we folded the lightcurves with the pre-glitch values of  $\nu$  and  $\dot{\nu}$ , obtaining a plot of the phase residuals with respect to the extrapolation of the pre-glitch solution ( $\nu_0$  below). The fit was then made through the formula:

$$\nu(t) - \nu_0(t) = \delta\nu_{exp} \exp\left(-\frac{t-t_g}{\tau}\right) + \Delta\nu_l + \Delta\dot{\nu}_l(t-t_g) + (1/2)\Delta\ddot{\nu}_l(t-t_g)^2 \quad (4)$$

with  $\phi(t) = \phi(t_g) + 2\pi \int_{t_g}^t [\nu(t') - \nu_0(t')] dt'$

The epoch of the glitch ( $t_g$ ) was fixed at the midpoint between the last pre–glitch and the first post–glitch observation.

The parameters of the best–fit exponential solution to glitch N.2 are also reported in Tab.2; these include a significant change in  $\dot{\nu}$  with respect to the pre–glitch solution while both  $\Delta\nu_l$  and  $\Delta\ddot{\nu}_l$  are fixed to zero. This because no significant improvement of the fit is obtained allowing also for changes of either parameters. However we report in Tab. 2 a 99.9% confidence interval for a possible  $\Delta\nu_l$ .

In glitch N.1 a good fit is obtained with either a step in  $\nu$  or in  $\dot{\nu}$ , while allowing for both does not prove statistically significant at the 99% confidence level.

Based on the  $\chi^2$  (or the r.m.s.) of the fits, the exponential recovery solutions do not provide a preferable description of the observations. However, at glitch N.2 the exponential model fits the evolution of the observed phases with a smaller set of parameters with respect to the polynomial expansion.

We note that very recently Kaspi & Gavriil (2003) have carried out a similar timing analysis of this source detecting glitch N.2 as well. Their results concerning this glitch are somewhat different from ours, since they assumed a step  $\Delta\nu_l \sim 1.3 \times 10^{-8}\text{s}^{-1}$  superposed to the exponential component and no significant change in  $\dot{\nu}$ . As they suggest, this apparent discrepancy is due to the non–inclusion of the  $\ddot{\nu}$ –term in their fit during the interglitch time, since this may be contaminated by timing noise. However the post–glitch N.1  $\Delta\dot{\nu}/\dot{\nu}$  they find is wholly unrecovered and amounts almost exactly to the unrecovered  $\Delta\dot{\nu}/\dot{\nu}$  ( $\sim 10^{-2}$ ) we found after glitch N.2. On the other hand,  $\dot{\nu}$  in our model for glitch N.1 is completely recovered and returned to its pre–glitch value right before the second glitch. Thus, the apparently different solutions do indeed agree in that the long–term  $\dot{\nu}$  after the second glitch is greater by  $\sim 1\%$  than its value previous to the first glitch (see Fig. 1, bottom panel of Kaspi & Gavriil 2003).

Concerning the nature of the interglitch  $\ddot{\nu}$ , we stress that its inclusion in the post–glitch N.1 model provides a great improvement of the fit to the phases. The  $\chi^2$  value changes from 72 (with 16 d.o.f.) to 11 (with 15 d.o.f.), which corresponds to a significance level greater than  $5\sigma$ . In the solution previous to glitch N.1 the significance of  $\ddot{\nu}$  was at the  $2.6\sigma$  level if the first data point, which deviated significantly from the average of all other points, was

excluded from the fit, and at less than  $4\sigma$  in any case (see Kaspi et al. 2000). From Fig. 2 of Kaspi & Gavriil (2003) the residuals with respect to their fits appear to increase with time, somewhat in connection with the occurrence of glitches, while we do not find any hints to such variations.

After both glitches we found small but statistically significant changes in the shape of the average pulse profile. The templates for each of the three intervals are shown in Fig. 4. Each of them was obtained after folding a reduced set of observations, namely only those in the corresponding interval that could be phase-connected with a simple  $(\nu, \dot{\nu})$  model. The adopted values of  $\nu$  and  $\dot{\nu}$  for the folding were those derived by the best-fit to this reduced set, instead of the global best-fit parameters. Though small, observed changes are statistically significant. The best-fit parameters for the three average pulse profiles are reported in Tab. 3. After glitch N.1 the average pulse-profile can still be fit with three harmonics, but changes in the amplitude ratios and phase differences are 3–5 times greater than reported  $1\sigma$  errors. On the other hand, after glitch N.2 a fourth harmonic becomes statistically significant ( $\chi^2 = 69.1$  with 59 d.o.f. and  $\chi^2 = 49.0$  with 57 d.o.f.) while the amplitude ratios and phase differences of the first three components are consistent with those determined previous to the glitch.

Short-duration bursts in the X-ray emission of two AXPs have been recently detected (Kaspi et al. 2002, Kaspi et al. 2003). Since the recently detected outburst in 1E2259+586 was also associated to a large glitch, we looked for bursts in the same X-ray lightcurves used for the phase-fitting. These were binned at 62 ms and only photons in the 2.5–6 keV range were selected, so our search was somewhat limited in sensitivity. Each lightcurve was searched for fluctuations above a significance threshold of  $8\sigma$  with respect to its mean count rate. No events were found above the threshold, so our data do not show evidence for bursts. Given the limitations discussed above the possibility of very short-term ( $t < 60$  ms) bursts cannot be ruled out.

## 5. A comparison of the two detected glitches

The most striking feature of the glitching behaviour of this source is the different appearance of the two spin-up events, in particular the remarkably different changes in  $\dot{\nu}$  and in the recovery timescales, both unusual findings compared to radio pulsars.

Following glitch N.1 the first derivative of the spin frequency ( $\dot{\nu}$ ) went back to its pre-glitch value at a constant rate (constant  $\ddot{\nu}$ ), over one year or so, with no significant exponential short-term component. Both the inferred changes  $\Delta\nu/\nu$  and  $\Delta\dot{\nu}/\dot{\nu}$  are in the

range of those observed in Vela–like glitches, where tipically  $\Delta\nu/\nu \sim 10^{-7} \div 10^{-6}$  and  $\Delta\dot{\nu}/\dot{\nu} \sim 10^{-3} \div 10^{-2}$ .

The recovery time  $\Delta t$  can be evaluated setting to zero the expression of the frequency difference between the post–glitch and the extrapolated pre–glitch solution:

$$\Delta\nu(t) = \Delta\nu_g + \Delta\dot{\nu}_g(t - t_g) + \frac{1}{2}\Delta\ddot{\nu}_g(t - t_g)^2 \quad (5)$$

where the subscript  $g$  indicates quantities evaluated at the assumed epoch of the glitch,  $t_g$ . It obtains  $\Delta t \sim 400$  d, to be compared with the  $\sim 600$  d one obtains for the recovery of  $\Delta\dot{\nu}_g$ . This discrepancy is not very significant however, given the uncertainty on  $\ddot{\nu}$  and on the extrapolated value of  $\nu$ . It can be concluded that  $\nu$  and  $\dot{\nu}$  have approximately relaxed back to their pre–glitch values over a timescale  $\sim 400$ – $600$  d. The constant second derivative measured after glitch N.1 may then represent a long–term linear recovery of  $\dot{\nu}$  towards its preglitch value. In this case, it is characterized by a timescale comparable – though somewhat shorter – to typical values ( $> 2$ – $3$  yrs) of radio pulsars with the same linear response.

Glitch N.2 is, on the other hand, quite different. The fractional spin–up  $\Delta\nu/\nu \sim 3 \times 10^{-6}$  is comparable to the giant glitches observed in the Vela and other pulsars of similar spin–down age and  $\Delta\dot{\nu}/\dot{\nu}$  is one of the largest observed ever. Comparable changes in the spin–down rate have been detected in a few giant glitches of the Vela pulsar (Lyne et al. 2000), but were followed by a fast recovery ( $\tau \leq 1$  day, Flanagan 1990). On the contrary, the recovery from glitch 2 of RXS J170849.0–400910 is found to last  $\sim 100$ – $200$  days. The only other long lasting ( $\sim 60$  d) large change in  $\dot{\nu}$  is the one recently observed in association with an X–ray outburst in the AXP 1E 2259+586 (Kaspi et al. 2003).

Residual arrival times of Fig. 2 show that, after glitch N.2, the source evolves towards a rotational period longer than the extrapolation of the pre–glitch solution. Indeed, had the recovering  $\nu(t)$  asymptotically approached the extrapolated pre–glitch solution from above, time residuals would have asymptotically settled towards a constant offset with respect to pre–glitch ones. This is a peculiar result, found rarely in other sources. One remarkable case is the Crab glitch of 1975 February 4 where, due to a persistent (at least for 3 yrs) fractional increase in the spin–down rate of the order  $\sim 10^{-4}$ , the spin frequency after the exponential recovery ( $\tau \sim 50$  d) became slower than expected from the pre–glitch solution (Link, Epstein and Baym, 1992). This is an interesting constraint on any model, indeed, and will be discussed in Sec. 6.2.

As already discussed in the previous section, the quick recovery from glitch N.2 suggests that a different function, such as the exponential decay of the kind given by Eq. (4), may be better suited to fit the observed phases.

However, in order to obtain an acceptably good fit for the recovery form glitch N.2, one must allow for a steepening of  $\dot{\nu}$  ( $\Delta\dot{\nu}_l/\dot{\nu} \simeq 9 \times 10^{-3}$ , where the denominator is the pre–glitch value of  $\dot{\nu}$  reported in Tab. 2) superposed to the exponentially recovered spin–up ( $\chi^2=18.45$  with 10 d.o.f.). Large recovery fractions and permanent increases in the spin–down rate are typical of the Crab pulsar glitches, but these are usually smaller events, with  $\Delta\nu/\nu < 10^{-7}$  and  $\Delta\dot{\nu}_l/\dot{\nu} < 10^{-3}$ . Thus differences and similarities with both Vela–like and Crab–like glitches are found in glitch N.2.

An alternative fit to the phases, with a step in  $\nu$  superposed to the exponential component and  $\Delta\dot{\nu}_l$  of Eq. (4) fixed to zero gave a worse fit ( $\chi^2=30.9$  with 10 d.o.f.). Finally, when both  $\Delta\nu_l$  and  $\Delta\dot{\nu}_l$  were left as free parameters, no significant improvement of the fit was obtained ( $\chi^2=17.71$  with 9 d.o.f.) with respect to the model above with  $\Delta\nu$  only.

The plots of the best–fit solution of Eq. (4) to the phase residuals after subtraction of the preglitch model and of time residuals with respect to this best–fit solution are shown in Fig. 5 and Fig. 6 respectively.

In conclusion, the recovery from glitch N.2 is consistent with an exponential decay with a timescale  $\tau \sim 50$  d. There is evidence for a steepening ( $\simeq 0.9 \%$ ) of the long–term spin–down rate as well, which is an order of magnitude greater than observed permanent changes in Crab–like glitches while comparable to changes recovered linearly over a few years in Vela–like glitches. Future observations will help revealing the possible long–term recovery of  $\Delta\dot{\nu}_l$  (a significant  $\dot{\nu}$ ) or a possible  $\Delta\nu_l$ , which here are found to be both non significant.

An exponential fit to the residuals of glitch N.1 after subtraction of the pre–glitch model required a further component superposed to the exponentially recovered spin–up ( $\tau \sim 350$  d), either a negative step in the frequency ( $\Delta\nu_l/\nu = (-3.9 \pm 0.7) \times 10^{-7}$ ) or an increase (in absolute value) of the first derivative ( $\Delta\dot{\nu}_l/\dot{\nu} = (3.1 \pm 0.6) \times 10^{-3}$ ). In either case one obtains similarly good fits (respectively  $\chi^2=13.7$  and  $13.47$  with 15 d.o.f.), while including both components provides no significant improvement of the fit. Stated differently, at glitch N.1 data do not allow an unambiguous determination of the exponential recovery solution (Eq. 4). Thus the polynomial solution for this glitch is still preferred.

## 6. Discussion

### 6.1. RXS J170849.0–400910 compared to radio pulsars

As a first step in the investigation of our results we compare them with some qualitative correlations between glitch variables studied by Lyne et al. (2000) in a sample of 48 radio

pulsar glitches.

It is usually assumed that glitches are a manifestation of the angular momentum exchange between the bulk of a neutron star's moment of inertia and some superfluid component, loosely coupled to it, that slows down at discrete steps. Let the spin-up rate associated with glitches be  $\dot{\nu}_{glitch} = (\sum_i \Delta\nu_i)/\Delta t$ , where the summation is over all glitches observed during the time  $\Delta t$ . Lyne et al.(2000) found a good correlation between the long-term spin-down rate of radio pulsars and  $\dot{\nu}_{glitch}$ . Their best-fit linear relation is:

$$\dot{\nu}_{glitch} = 1.7 \times 10^{-2} \dot{\nu} \quad (6)$$

In the framework discussed above, conservation of total angular momentum and eq. (6) imply that a fraction  $\sim 1.7 \times 10^{-2}$  of the moment of inertia of the star is on average contributed by the superfluid that is slowed down at glitches (see Sec. 6.2).

In the case of the two glitches observed in RXS J170849.0–400910  $\dot{\nu}_{glitch} \sim 2.6 \times 10^{-15} \text{ s}^{-2}$ , which is strikingly close to the value ( $2.7 \times 10^{-15} \text{ s}^{-2}$ ) predicted by formula (6). We stress however that this result still needs a confirmation, being based on only two events.

Further, the polynomial fit to the recovery from glitch N.1 is consistent with the trend observed in radio pulsars for rotators with decreasing  $\dot{\nu}$  to have smaller exponential recovery fractions ( $Q$ ) and increasingly important long-term linear recoveries. Based on such observed trend a recovery fraction  $Q \sim 10^{-3}$  would be expected for RXS J170849.0–400910 (see Fig.6 of Lyne et al. 2000). A short-time transient of this magnitude cannot be excluded given the sparse temporal monitoring of this source.

On the other hand, the trend is contradicted by the exponential fit to the recovery from glitch N.2. This is dominated by an exponential component ( $Q \sim 1$ ). Recovery fractions greater than 10% have been found only in the fastest and youngest (the Crab pulsar) and in the slowest and oldest (PSR B0525+21) radio pulsars in the sample of Lyne et al. (2000). AXPs do likely spin-down under different conditions with respect to common radio pulsars and may have higher temperatures than radio pulsars of the same spin-down age. Both effects may be relevant in determining the properties of their recovery from glitches.

We notice that two other suggestions made by Lyne et al.(2000) do not fit with what is observed in RXS J170849.0–400910; the tendency for stars with a lower rotational frequency to experience, if any, glitches of smaller amplitude and, second, the tendency for stars with a higher dipole field to show more frequent but smaller glitches, at a given characteristic age. Indeed, the average  $\Delta\nu/\nu$  of the two observed glitches amounts to  $\sim 2 \times 10^{-6}$ , very close to the value of the Vela pulsar ( $\sim 1.7 \times 10^{-6}$  as derived from Tab. 3 of Lyne et al. 2000).

Thus, though the average amplitude of the glitches in 1RXS J170849.0–400910 and the interglitch time are consistent with those found in radio pulsars of comparable spin–down age (particularly with those of the Vela pulsar), looking more closely at the results one finds peculiarities difficult to account for.

First, the average glitch amplitude and the short interglitch time are unexpected, since slow rotators do on average experience glitches of smaller amplitude and less frequently. This result may rule out a clear dependence on the rotation period and suggest that the main role could be played by the age of the neutron star. Indeed, contrary to radio pulsars with comparable rotational frequency, AXPs are slow but relatively young rotators.

Second, a fractional increase of  $\dot{\nu}$  as high as  $\sim 30\%$ , and with a relatively long recovery timescale (tens to hundreds days) has never been observed in glitching radio pulsars. The only other source with such an anomalous behaviour is 1E 2259+586, in which the glitch recently detected produced a change of  $\sim 100\%$  in the spin first derivative, recovered over  $\sim 60$  d (Kaspi et al. 2003). The fact that both glitching AXPs, and only them, have displayed such changes of  $\dot{\nu}$  after a glitch hints to an AXP mechanism triggering more extreme events than in radio pulsars, but a larger sample of glitches and of sources is needed to check this possibility.

Finally, one may explain the high fractional change of  $\dot{\nu}$  if the recovery in glitch N.2 is modeled as an exponential. Even in this case, however, a problem is presented by the very smooth and linear recovery seen after glitch N.1; the star appears to have undergone an important change in its dynamical response over the short time interval elapsed between the two glitches. A way out may be assuming that the two events have been triggered by two different mechanisms, a possibility that will be discussed along with others in the following sections.

## 6.2. Vortex creep model applied to RXS J170849.0–400910

It is generally assumed that neutron–rich nuclei in the inner crust of a neutron star act as pinning centers for the vortices created by the superfluid in response to the rotation of the star (Andersson & Itoh 1975).

The superfluid can follow the crust’s spin–down by outward migration of vortices, which is impeded by the pinning energy barrier. In vortex creep model (Alpar et al. 1984, 1989, 1993) the rotational lag ( $\omega = \Omega_{sf} - \Omega_c$ ) that develops between the crust (spinning at  $\Omega_c$ ) and the superfluid (spinning at  $\Omega_{sf}$ ) causes a Magnus force to arise, so that vortices overcoming the pinning energy barrier through thermal activation are driven outwards by this force,

establishing a continuous vortex current through which the superfluid spins down. In doing so, it exerts an internal spin-up torque on the crust opposed to the magnetic braking. Eventually a steady-state is reached in the relaxation time  $\tau$ , when both the crust and the superfluid spin-down at the same rate ( $\dot{\Omega}_\infty$ ) with a steady-state lag  $\omega_\infty$ , subject to the external torque  $N_{ext}$ .

In steady-state, the equation of motion is simply:

$$(I_c + I_{sf})\dot{\Omega}_\infty = N_{ext} \quad (7)$$

A glitch results from an instability of the steady-state. Inhomogeneities of the pinning force throughout the crust determine a non uniform distribution of vortices: local values of  $\Omega_{sf}$  will be enhanced by accumulation of vortices until a critical lag  $\omega_{cr}$  is reached, beyond which an avalanche unpinning of vortices occurs and angular momentum is transferred to the crust. Relaxation to the new steady-state will determine the post-glitch recovery. The value of  $\omega_{cr}$  determines whether the pinning is strong or weak. At the high density of the deep crust a change in the nature of pinning is thought to occur, bringing it to a superweak regime, even though this conclusion is not testable in terrestrial materials.

The conservation of total angular momentum during the glitch gives (Alpar et. 1993, Alpar 2000):

$$(\alpha I_A + I_B)\delta\bar{\Omega} = I_c\Delta\Omega_c \quad (8)$$

where  $I_A + I_B = I_{sf}$  is the moment of inertia of the pinned superfluid,  $\delta\bar{\Omega}$  is its change in rotational frequency and the right hand side refers to the crust plus all matter components coupled to it on very short timescales: these include the bulk of the core material (Alpar, Langer and Sauls 1984) which makes up most of the moment of inertia of the star. Two different situations may occur in the crustal superfluid: in type-A (accumulation) regions unpinning takes place, vortices move outwards and repin in another type-A region. For a uniform density of unpinned vortices  $\alpha = \frac{1}{2}$  ( $0 < \alpha < 1$  in general).

Type-B regions exist between accumulation zones and are vortex-depleted regions. Thus they are decoupled from the crust and spin-down only at glitches, when a net outward flux of vortices crosses them. Thus they contribute to  $\Delta\Omega_c$  at the glitch but not to changes in  $\dot{\Omega}_c$ .

The relaxation time  $\tau$  depends on whether the response of the superfluid to the initial perturbation of the lag,  $\delta\omega(t = 0)$ , is linear or non linear. The corresponding expressions are (Alpar et al. 1989):

$$\tau_l = \frac{kT}{E_p} \frac{\omega_{cr} r}{4\Omega v_0} \exp\left(\frac{E_p}{kT}\right) \quad (9)$$

$$\tau_{nl} = \frac{kT}{E_p} \frac{\omega_{cr}}{|\dot{\Omega}|_\infty} \quad (10)$$

in the linear and non linear regime, respectively. The former situation will occur when  $\omega_\infty \ll \omega_{cr}$ , the latter when the steady-state is close to the condition for unpinning,  $\omega_\infty \leq \omega_{cr}$ . The system will always be in the regime with the shortest time, so a transition value for  $(E_p/kT)$  can be found by equating the two (Alpar et al. 1993). For RXS J170849.0–400910 it obtains  $(E_p/kT)_{cr} \simeq 30.8$ . If the ratio is below this limit the superfluid responds linearly, while non-linearity corresponds to a value higher than critical.

The non-steady-state equivalent of eq.(7) in the linear and non linear regime are, respectively (Alpar et al. 1989):

$$\dot{\Omega}_c = \dot{\Omega}_\infty - \frac{I_{sf}}{I_c} \frac{\delta\omega(0)}{\tau_l} \exp\left(-\frac{t}{\tau_l}\right) \quad (11)$$

and

$$\dot{\Omega}_c = \frac{I}{I_c} \dot{\Omega}_\infty - \frac{I_{sf}}{I_c} \dot{\Omega}_\infty \frac{1}{1 + [\exp(t_0/\tau_{nl}) - 1] \exp(-t/\tau_{nl})} \quad (12)$$

where  $t_0 = \frac{\delta\omega(0)}{|\dot{\Omega}|_\infty}$  is an offset time indicating how long, after the decoupling, the region of interest will start recoupling through creep.

In the linear regime an exponential recovery is expected while nonlinear regions have a more complex response. With  $\alpha=(1/2)$  and  $\tau_{nl} < (t_0)_{max} = \frac{\delta\bar{\Omega}}{|\dot{\Omega}|_\infty}$ ,  $\dot{\Omega}_c$  will recover linearly in time due to the progressive recoupling of type-A regions.

Glitch N.1 has been previously interpreted in terms of a non-linear response. If most of the superfluid had been involved in vortex motion (then  $I_B \ll I_A$ ), a fraction  $1.72 \times 10^{-2}$  of the whole moment of inertia of the star needs to be contributed by the pinned superfluid. The expected time to the next glitch is then  $t_g \sim (t_0)_{max} \simeq 500$  days (a smaller value ensues if allowance for a significant  $I_B$  is made), remarkably close to the measured interval of 550 days. For the recovery to be linear in time it is required that  $\tau_{nl} < t_g$ , implying  $\omega_{cr} < 4.3 \times 10^{-5} (E_p/kT) < 10^{-2} \text{rad s}^{-1}$  even for the largest values of the ratio  $(E_p/kT)$ .

From Eq.(8) and the glitch amplitude in Tab.1 one gets  $\delta\bar{\Omega} \leq 4.2 \times 10^{-5} \text{rad s}^{-1}$ . The condition (Alpar et al. 1989)  $\omega_{cr} > \delta\omega \simeq \delta\bar{\Omega}$  for the non-linear regime thus gives the lower bound  $\omega_{cr} > 4 \times 10^{-5} \text{rad s}^{-1}$ . A non linear regime obtains only for a very low value

of  $\omega_{cr}$ , requiring superweak pinning throughout most of the crust. This is surprising since superweak pinning should characterize the innermost and densest layers of the crust.

The change in  $\dot{\nu}$  measured in glitch N.2 cannot arise from a non-linear response. The fractional change in  $\dot{\nu}$  in this regime is always less than the ratio  $(I_{sf}/I_c)$  (Eq.12), thus an unreasonably high moment of inertia of the superfluid would be implied. Only the linear response (and consequently an exponential recovery) of a region where unpinning did take place ( $\delta\omega \simeq \delta\bar{\Omega}$ ) can account for such a high fractional change. If the two glitches were due to the same mechanism, the recovery from glitch N.1 should be modeled as an exponential as well or one should invoke a change in the response regime of the superfluid.

In the case of two exponential recoveries, the different timescales hint to the association of the two glitches with different regions of the superfluid. In particular, they must reflect the different values of  $\omega_{cr}$  or  $E_p$ . The value of  $\tau_l$  is very sensitive to the ratio  $(E_p/kT)$  (Eq.9), so that a difference of a factor  $\sim 6$  can arise from a small difference in that ratio. Since both recoveries are fit with only one of the two exponential components, these must have unpinned alternately. Stated differently, the possibility of local unpinning should be introduced in the model.

The shorter recovery timescale of glitch N.2 would require a smaller  $\omega_{cr}$  or a lower  $(E_p/kT)$ , corresponding to a region of weaker pinning, given the same response regime. In particular, the smaller value of  $\omega_{cr}$  would imply a correspondingly larger fraction of superfluid to have unpinned, in order to produce the larger glitch N.2.

Glitch N.1 may have originated in the outer layers of the crust, where  $\omega_{cr}$  is likely higher, leaving the more weakly pinned, inner superfluid unperturbed (apart from the very small  $\Delta\Omega_c \sim 4 \times 10^{-7}$  rad s $^{-1}$ ). The roles of the two components should be interchanged to explain glitch N.2. Anyway, in vortex creep model unpinning is a widespread rather than local mechanism (Pines 1999, Jones 2002), so this would be an ad hoc assumption.

If one modeled the recovery from glitch N.1 as a linear decay, a change in the response regime of at least some parts of the superfluid must have occurred over the  $\sim 500$  days of interglitch time. This may happen if after glitch N.1, where the response was non linear, a significant release of heat acted to decrease the ratio  $E_p/kT$ , bringing the latter below the transition value. However, such a heat release would require some new mechanism not included in vortex creep model (*e.g.* a starquake, see Sec. 6.4).

Furthermore, as already discussed in Sec. 4, the period evolution after glitch N.2 is unusual. After the initial recovery of the spin-up, the spin frequency becomes lower than expected from the extrapolation of the pre-glitch solution. In the exponential fit this effect is due to the unrecovered increase in the long-term spin-down rate. Link, Epstein and Baym

(1992) have shown that in vortex creep model, where no explicit temporal dependence of the net (external+internal) torque acting on the crust is included, the post-glitch spin frequency must always remain higher than the extrapolation of the pre-glitch value, approaching it in the long run. Thus Fig. 2 argues against an interpretation of glitch N.2 in terms of vortex creep model, unless allowing for a change in the torque, either external or internal, induced by the glitch.

In summary, one needs a contrived interpretation in order to account for the different amplitudes and recoveries of the two observed glitches within the framework of vortex creep model. In fact one should assume the two glitches to be produced by different mechanisms, thus attributing the different recoveries to the response of the star to different kinds of perturbation.

### 6.3. Core superfluid models

One of the basic assumptions of crustal superfluid models is that the core neutron superfluid be strictly coupled to 'the protons' (the star's crust, core superconducting protons and degenerate electrons) on the timescales of post-glitch recoveries. The coupling is provided by scattering of the electrons – following the crust spin – off magnetic flux tubes that thread neutron vortex cores as a result of the entrainment-induced circulation of superconducting protons around them (Alpar, Langer and Sauls 1984, Prix et al. 2002). It has been suggested (Andersson and Comer 2001, Andersson et al. 2002, Sedrakian & Sedrakian 1995) that the above assumption may be questionable, as the coupling time  $\tau_c \propto (c_r + c_r^{-1})$  between neutron vortices and 'protons' depends on the uncertain parameter  $c_r$ , the ('drag-to-lift') ratio between the drag force due to entrainment and the Magnus force, both acting on neutron vortex lines in the decelerating core. From the above expression,  $\tau_c$  is found to be smallest for  $c_r \sim 1$ , while in both cases of weak ( $c_r \ll 1$ ) and strong ( $c_r \gg 1$ ) coupling,  $\tau_c$  can increase significantly.

Andersson et al. (2002) studied a two-superfluid instability that may take place in the core of neutron stars if a rotational lag between the superfluid neutrons and 'the protons' can develop, due to a long coupling time. The instability triggers a sudden rearrangement of the neutron vortex distribution in an outer core shell, leading to a glitch. In this model a simple formula is given to estimate the interglitch time  $t_g$  in RXS J170849.0–400910. The instability takes place when the rotational lag ( $\omega$ ) between the two components is large enough to overcome the coupling due to the drag force ( $\omega > \omega_{cr}$ ). Thus:

$$t_g = 2t_s \frac{\omega_{cr}}{\Omega_c} \quad (13)$$

where  $\omega_{cr}$  has an analogous meaning as it has in vortex creep model while  $t_s$  is the spin-down age of the star.

Assuming  $\omega_{cr} \simeq 5 \times 10^{-4} \text{ rad s}^{-1}$  as a typical value of the lag for unpinning (Andersson et al. 2002 and references therein), no glitch would be expected within  $\sim 30$  years after glitch N.1. Thus, for this model to apply to RXS J170849.0–400910, a very low value of  $\omega_{cr} \leq 3 \times 10^{-5} \text{ rad s}^{-1}$  would be required. Whether such a low value still allows the lag to effectively develop is an open question.

An attractive feature is that, if 30 yrs did represent the characteristic recurrence time for the core instability in 1RXS J170849.0–400910, this model would allow a natural interpretation of the different properties of the two observed glitches, since these could not be due to the same mechanism. In particular, if glitch N.2 was due to this instability, a substantial fraction of the core superfluid could have decoupled, thus explaining the large increase of  $\dot{\nu}$  as a significant reduction in the moment of inertia acted on by the braking torque. The different responses and recovery timescales of the two glitches would be – at least qualitatively – accounted for, since in glitch N.2 they would reflect mainly the dynamical relaxation of the core rather than crustal superfluid.

Thus two different glitch mechanisms could be at work in the same source. Future timing observations will help testing this interesting possibility, as more glitches are expected. Since it may take more than a decade for a new event similar to glitch N.2 to occur, the lack of such events in the next years may indeed provide an indirect hint to the viability of this picture.

#### 6.4. The starquake scenario

It has been recently shown (Wang et al. 2000) that most glitch models are difficult to reconcile with observations of a growing number of glitches. All models requiring a catastrophic (*i.e.* widespread) unpinning of crustal superfluid require simple correlations between the amplitudes and recovery timescales of glitches in a single source as well as an approximately constant Q-value, which is found not to be the case, in general. This is the same difficulty met in Sec. 6.2 for the two glitches of 1RXS J170849.0–400910. We suggested the possibility that these events were due to a local, rather than global, release of angular momentum. This is the same conclusion of Wang et al.(2000) based on a sample of 30 glitches.

An entirely different explanation with respect to those discussed previously has been proposed for at least the large glitches of radio pulsars: these may be associated to starquakes and subsequent movements of cracked platelets (Ruderman 1991, Ruderman, Zhu and Chen 1998, Epstein and Link 2000). Several cracking mechanisms have been proposed for radio pulsars; quakes have been ascribed to the stress acted on the crust by the interaction in the core between superfluid neutrons and magnetic flux tubes threading the crust (Ruderman, Zhu and Chen 1998). Alternatively, the growing strain in the crust of a spinning-down neutron star may fracture it due to the resulting shear stress (Franco, Link and Epstein 2000). Whatever the trigger, the movement of a sector of the crust with its frozen-in magnetic flux can cause an increase of the angle  $\alpha$  between the rotation and magnetic axis and a subsequent increase of the braking torque exerted on the star.

The most important feature of this scenario is its local nature; only the moving sector and its surroundings are affected leaving the rest of the star mainly unperturbed (Jones 2002). Further, following a starquake, a permanent increase of  $\dot{\nu}$  could result as a consequence of the net increase in the braking torque. A residual torque increase has indeed been observed after several glitches in the Crab pulsar which may result from permanent changes in the magnetic torque (Link, Epstein and Baym 1992, Link & Epstein 1997). Our exponential fit to the recovery from glitch N.2 provides evidence for an increase in the spin-down rate, though greater than those observed in the Crab pulsar. Whether this increase is recovered over a timescale longer than 1 yr or not is a crucial question to be answered only with future observations. In vortex creep model this change would be attributed to some of the pinning layers responding non linearly to the glitch and recovering over a time  $t_g = \delta\omega/|\dot{\Omega}|_\infty$ . If vortices did unpin in these layers a linear recovery of  $\dot{\nu}$  is expected, while if they did not unpin  $\delta\omega = \Delta\Omega_c$  and a step-like (Alpar et al. 1984) recovery of  $\dot{\nu}$  would occur, after a waiting time  $t_0 = \Delta\Omega_c/|\dot{\Omega}|_\infty$ . On the other hand, finding no significant recovery of  $\Delta\dot{\nu}_l$  in future observations would be in agreement with the expectations from plate tectonics.

In the model by Ruderman, Zhu and Chen (1998) glitch activity is expected to cease at rotational periods  $P > 0.7$  s because of the decreasing pull of core neutron vortices on flux tubes. Thus an intrinsically different mechanism would be required to cause starquakes in slow rotators such as AXPs. In the case of shear stress-induced fractures, the high spin-down of AXPs may well produce starquakes. Although it has been proved to be impossible on energetic grounds to account for the frequent glitches (every  $\sim 2$  yrs) of the Vela pulsar through this mechanism (Sauls 1988 and references therein), we stress that a Vela-like glitch in an AXP ( $\Delta\nu/\nu \sim 10^{-6}$ ) will involve some 4 orders of magnitude less energy ( $\Delta E \propto \nu^2$ ). Thus the energetic argument may still leave room for spin-down-induced glitches in AXPs. However AXPs in the magnetar model are candidates for starquakes triggered by a peculiar mechanism (Thompson and Duncan 1996). The super strong magnetic field diffusing through

the core can induce stresses in the crustal lattice strong enough to crack it. A range of length scales for magnetically–driven fractures is expected; continuous small scale fracturing is produced by the diffusion of the field through the crust while larger scales, comparable to the thickness of the crust, are likely involved by sudden rearrangements of the field distribution. When the crust yields, the sudden shaking of magnetic footpoints excites magnetospheric Alfvèn waves; in particular, burst–like enhancements of the X–ray emission are expected in association with larger scale fractures. This mechanism has been proposed to explain the repeat bursts of Soft Gamma Repeaters (Thompson & Duncan 1993) and may be relevant also to AXPs. Indeed, the simultaneous occurrence of a major X–ray outburst and a large glitch in the AXP 1E2259+86 (Kaspi et al. 2003) has provided a strong hint in favour of this interpretation. On the other hand, observations of burst activity in SGRs have revealed no clear correlation with glitch–like changes in the rotational parameters of the sources (Woods et al. 2002, 2003), making the interpretation of such effects still controversial.

Though the mechanism for cracking the crust may be different in AXPs and radio pulsars, the post–starquake evolution is likely to be similar, if determined mainly by the dynamical coupling of the superfluid components to crustal matter. Jones (2002) has investigated the post–glitch evolution of a neutron star following a starquake, taking into account the responses of both superfluids in the crust and the core. In that picture several physical parameters determine the mutual interaction between the superfluid components and the magnetic field and the interaction of crustal vortex lines with crustal nuclei. The location at which the fracture occurs is a key element, determining the relative importance of such parameters. A variety of glitch amplitudes, recovery fractions and timescales is expected not only in different sources but also in a single one, as fractures with different dimensions and at different depths would occur.

As a general remark, the complexity of the model and its dependence on poorly known parameters make predictions, if any, and quantitative observational tests very difficult. On the other hand, its complex nature makes it more suited than other models to the description of a variety of different glitches. In particular, the two glitches of RXS J170849.0–400910 do require a complex picture – if not ad hoc assumptions – even within other models. In the starquake scenario the two glitches would be explained assuming that the cracking and platelet movement did happen at two different locations within the crust. The unrecovered increase in the spin–down rate ( $\leq 1\%$ ) of glitch N.2 could then be attributed to a permanent change in the braking torque. This would require a change in the inclination angle between the magnetic and rotation axes  $\Delta\alpha \leq 10^{-2}\tan\alpha$ , actually a large value compared to expected ones ( $\leq 10^{-3}$ , Ruderman, Zhu and Chen 1998). Finally, a change in the magnetic field orientation would be expected to produce some changes in the shape of the pulse profile (Franco, Link and Epstein 2000), such as those we may have found here, particularly after

glitch N.2.

## 7. Conclusions

We have obtained a timing solution for 1RXS J70849.0–400910 spanning more than 4 years. We detected a new large glitch, whose characteristics place this source among the most frequent glitchers, undergoing large amplitude spin-ups.

The two glitches are perhaps an indication of yet another peculiarity of AXPs. Indeed, the source has experienced two large glitches followed by very different recoveries, the larger being recovered more quickly.

Our results allow for the first time a comparison between the glitch activity of an AXP and that of radio pulsars, an important step in the assessment of the nature of AXPs as extremely magnetised, isolated neutron stars. Our observations show that:

1. The short interval ( $t_g < 2$  years) between the two glitches of 1RXS J170849.0–400910 is comparable to the intervals found in the Vela pulsar, one of the most frequent glitchers. The two observed spin-ups are large, with average amplitude  $\Delta\nu/\nu \sim 2 \times 10^{-6}$  comparable to those of Vela and other so-called 'adolescent' pulsars (Lyne et al. 2000).
2. The average glitch-induced spin-up torque is comparable to that of the Vela pulsar and consistent with that found in radio pulsars of age  $t_s > 10^4$  yrs and with high enough  $\dot{\Omega}$  (Lyne et al. 2000).
3. The large average glitch amplitude ( $\sim 2 \times 10^{-6}$ ) is at variance with what observed in slow rotators, that appear on average to suffer rarer and smaller glitches. If one assumes AXPs to be magnetars, the large amplitude of the glitches is also at variance with the tendency for higher magnetic field neutron stars to experience smaller (but more frequent) glitches, at a given age (Lyne et al. 2000).
4. The two glitches are characterized by different types of recovery. The change in the rotational parameters after the second glitch is similar, though less extreme, than the recently detected burst-associated glitch in the AXP 1E 2259+586 (Kaspi et al. 2003).
5. There is evidence that the second glitch consisted of a large spin-up recovered exponentially over  $\sim 50$  d plus a steepening of the spin-down rate of the order of  $\sim 0.9\%$ . Further components, though non significant in the fits yet, cannot be ruled out. A

similar interpretation may hold for glitch 1 even though, in this case, data are wholly consistent with a simple linear recovery.

The two different recoveries are puzzling. No simple model can account for this finding and ad hoc assumptions would be required.

Observations do not seem to fit with models based only on instabilities of the crustal superfluid, such as vortex creep model. Indeed the recoveries have variable parameters from one glitch to the other, which would either require unpinning to occur in separate localized regions at each glitch or changes in the response regime of parts of the superfluid. Further, while an interpretation of glitch N.1 in terms of a non linear response within vortex creep model is perfectly consistent with observations, new hypotheses should be introduced in order to explain the decrease, observed after glitch N.2, of the rotational frequency below the extrapolation of the pre-glitch value.

A likely picture is that the two glitches were triggered by two different mechanisms. Models invoking a perturbation in the core superfluid may fit the properties of glitch N.2, in particular the inferred large change of  $\dot{\nu}$ . Further, in this case the long expected interglitch time would naturally lead to the conclusion that glitch N.1 could not be due to the same mechanism and provide a key to understanding the two different recoveries.

However, starquake models seem more promising. In general, their local nature and the complex picture of the glitch phenomenon that they provide seem to fit well with observations of a great variety of glitches in radio pulsars. Concerning AXPs, the glitch recently detected in 1E2259+586 is similar to glitch N.2 of 1RXS J170849.0–400910, having a comparable magnitude in  $\Delta\nu$  and an even greater change in  $\dot{\nu}$ . Put together, these two events may suggest that a peculiar glitch mechanism be at work in AXPs. In the magnetar model this might be associated to crustal cracking and/or plastic flow induced by the diffusing magnetic field. Indeed, the simultaneous outburst and glitch of 1E 2259+586 do provide a first strong hint that crust cracking–induced glitches can occur in AXPs, reinforcing a similar interpretation at least for glitch N.2 observed here, given their overall similarity. Though we found no evidence for bursts in 1RXS J170849.0–400910, our sensitivity to very short and hard events was limited. Moreover, both glitches did take place during  $\sim 40$ d time intervals between subsequent observations, so no firm conclusions about this point can be drawn. Finally, since no clear correlation between glitch and burst activity has been found in SGRs, it seems that observing them together may be the exception rather than the rule.

In the case of 1RXS J170849.0–400910, a starquake interpretation can account for the observed decrease, at glitch N.2, of the rotational frequency of the source below the extrapolation of the pre-glitch solution and also for the small, though significant, changes in the

average shape of the pulse profile, particularly after glitch N.2. On the other hand, starquake models involve many degrees of freedom and have, up to now, poor predictive power. More developments in modeling these events are needed in order to closely match them with observations. Further, future observations are needed in order to get a clearer picture of the glitch phenomenon in AXPs.

This work was partially supported by University of Rome “La Sapienza”.  
S.D. would like to thank the anonymous referee for helpful comments to the paper.

## REFERENCES

Alpar, M. A., Pines, D., Anderson, P. W., & Shaham, J. 1984, *ApJ*, 276, 325

Alpar, M. A., Langer, S. A., & Sauls, J. A. 1984, *ApJ*, 282, 533

Alpar, M. A., Cheng, K. S., & Pines, D. 1989, *ApJ*, 346, 823

Alpar, M. A., Chau, H. F., Cheng, K. S., & Pines, D. 1993, *ApJ*, 409, 345

Alpar, M. A. 2001, *ApJ*, 554, 1245

Anderson, P. W. & Itoh, N. 1975, *Nature*, 256, 25

Andersson, N. & Comer, G. L. 2001, *Classical and Quantum Gravity*, 18, 969

Anderson, N., Comer, G. L., Prix, R. 2002 [astro-ph/0211151](#)

Chatterjee, P., Hernquist, L., & Narayan, R. 2000, *ApJ*, 534, 373

Epstein, R. I., & Link, B. 2000 [astro-ph/0001365](#)

Flanagan, C. S. 1990, *Nature*, 345, 416

Franco, L. M., Link, B., & Epstein, R. I. 2000, *ApJ*, 543, 987

Gavriil, F. P., Kaspi, V. M., & Woods, P. M. 2002a, *Nature*, 419, 142

Gavriil, F. P. & Kaspi, V. M. 2002b, *ApJ*, 567, 1067

Hulleman, F., Tennant, A. F., van Kerkwijk, M. H., Kulkarni, S. R., Kouveliotou, C., & Patel, S. K. 2001, *ApJ*, 563, L49

Israel, G. L., Covino, S., Stella, L., Campana, S., Haberl, F., & Mereghetti, S. 1999, *ApJ*, 518, L107

Israel, G. L. et al. 2002, *ApJ*, 580, L143

Israel, G. L. et al. 2003, *ApJ*, 589, L93

Jones, P. B. 2002, *MNRAS*, 335, 733

Kaspi, V. M., Lackey, J. R., & Chakrabarty, D. 2000, *ApJ*, 537, L31

Kaspi, V. M., Gavriil, F. P., Chakrabarty, D., Lackey, J. R., & Muno, M. P. 2001, *ApJ*, 558, 253

Kaspi, V. M., Gavriil, F. P., Woods, P. M., Jensen, J. B., Roberts, M. S. E., & Chakrabarty, D. 2003 astro-ph/0304205

Kaspi, V. M., Gavriil, F. P. 2003 astro-ph/0307225 v2

Kern, B. & Martin, C. 2002, Nature, 417, 527

Link, B., Epstein, R. I., & Baym, G. 1992, ApJ, 390, L21

Link, B. & Epstein, R. I. 1997, ApJ, 478, L91

Lyne, A. G., Shemar, S. L., & Smith, F. G. 2000, MNRAS, 315, 534

Mereghetti, S. & Stella, L. 1995, ApJ, 442, L17

Mereghetti, S., Chiarlone, L., Israel, G. L., & Stella, L. 2002, Neutron Stars, Pulsars, and Supernova Remnants, 29

Pines, D. 1999, Pulsar Timing, General Relativity and the Internal Structure of Neutron Stars, 199

Prix, R., Comer, G. L., & Andersson, N. 2002, A&A, 381, 178

Ruderman, M. 1991, ApJ, 382, 587

Ruderman, M., Zhu, T., & Chen, K. 1998, ApJ, 492, 267

Sedrakian, A. D. & Sedrakian, D. M. 1995, ApJ, 447, 305

Sauls, J.A., 1989 *Timing Neutron Stars*, 457–490 H.Ögelman and E.P.J. van den Heuvel (eds.)

Thompson, C. & Duncan, R. C. 1995, MNRAS, 275, 255

Thompson, C. & Duncan, R. C. 1996, ApJ, 473, 322

van Paradijs, J., Taam, R. E., & van den Heuvel, E. P. J. 1995, A&A, 299, L41

Wang, N., Manchester, R. N., Pace, R. T., Bailes, M., Kaspi, V. M., Stappers, B. W., & Lyne, A. G. 2000, MNRAS, 317, 843

Woods, P. M. et al. 1999, ApJ, 524, L55

Woods, P. M., Kouveliotou, C., Göğüş, E., Finger, M. H., Swank, J., Markwardt, C. B., Hurley, K., & van der Klis, M. 2002, ApJ, 576, 381

Woods, P.M., Kouveliotou, C., Göğüş, E., Finger, M.H., Feroci, M., Mereghetti, S., Swank, J.H., Hurley, K., Heise, J., Smith, D., Frontera, F., Guidorzi, C., & Thompson, C. 2003 astro-ph/0306092

### Figure Captions

**Figure 1** — Time residuals of the pre–glitch model for observations between 1998 January 12 (MJD 50825) and 1999 September 25 (MJD 51446)

**Figure 2** — Time residuals of observations from 1999 October 21 (MJD 51472) to 2001 May 29 (MJD 52423) after subtraction of the post–glitch model N.1. The sharp increase (in absolute value) of the residuals between 2001 March 27(MJD 51995) and 2001 May 6 (MJD 52035) indicates the occurrence of glitch N.2. The vertical line corresponds to the assumed epoch of the glitch.

**Figure 3** — Time residuals of observations from 1999 October 21 (MJD 51472) to 2002 May 29 (MJD 52423) after subtraction of post–glitch model N.1 previous to May 2001 and the polynomial post–glitch model N.2 after (see Tab.2 for parameters). The vertical line indicates the assumed epoch of the glitch.

**Figure 4** — Average pulse–profiles for the three intervals of Tab. 3, from top to bottom Interval 1, 2 and 3.

**Figure 5** — Phase–residuals of the observations from 2001 May 6 to 2002 May 29 relative to the preglitch model (left column in Tab.2). The 0 in the abscissa is the assumed epoch of the glitch (MJD 52015.65).

**Figure 6** — Time residuals of the recovery from glitch N.2 (2001 May 6 – 2002 May 29) relative to the best–fit exponential+linear term of Eq. 4.

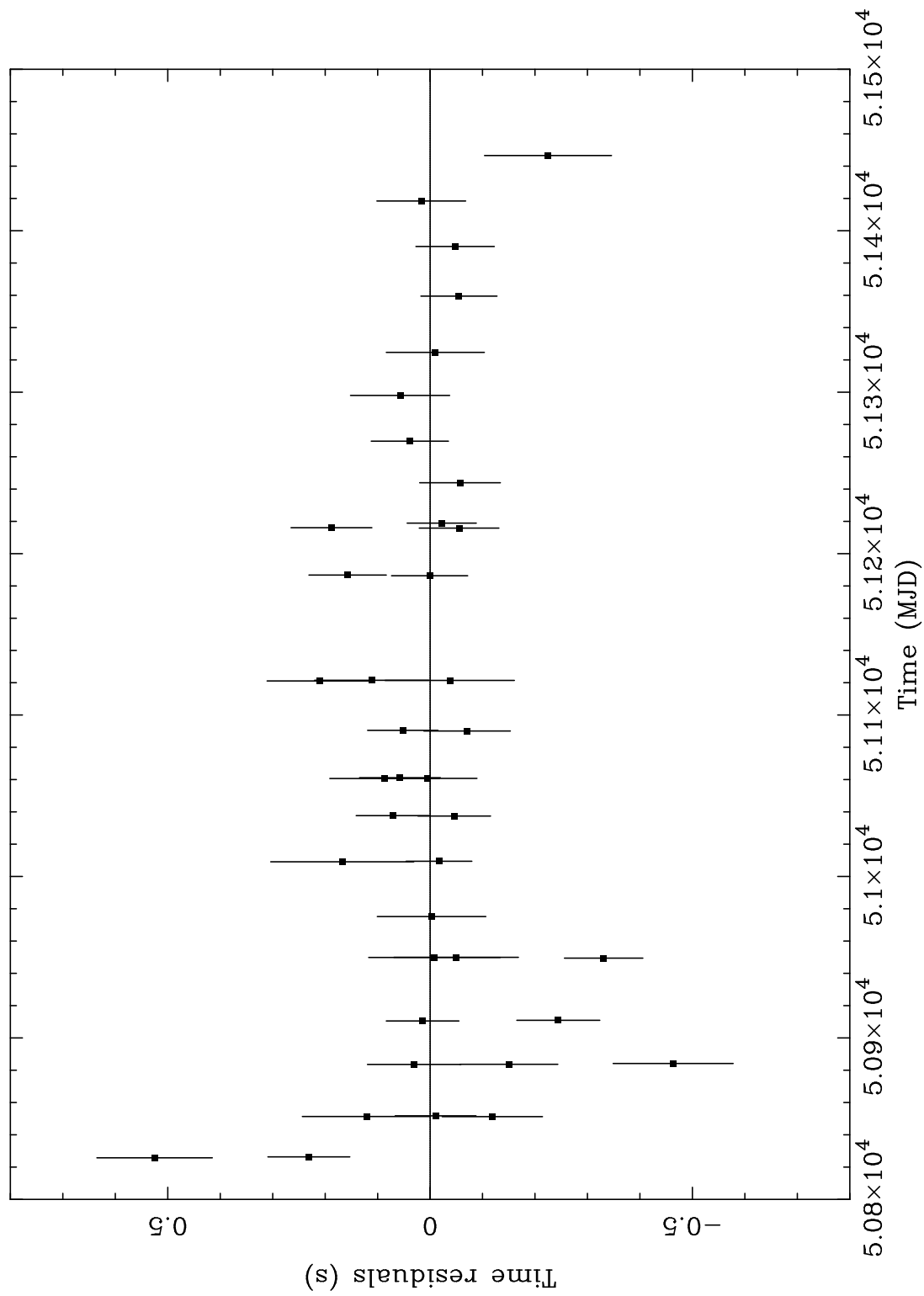


Fig. 1.—

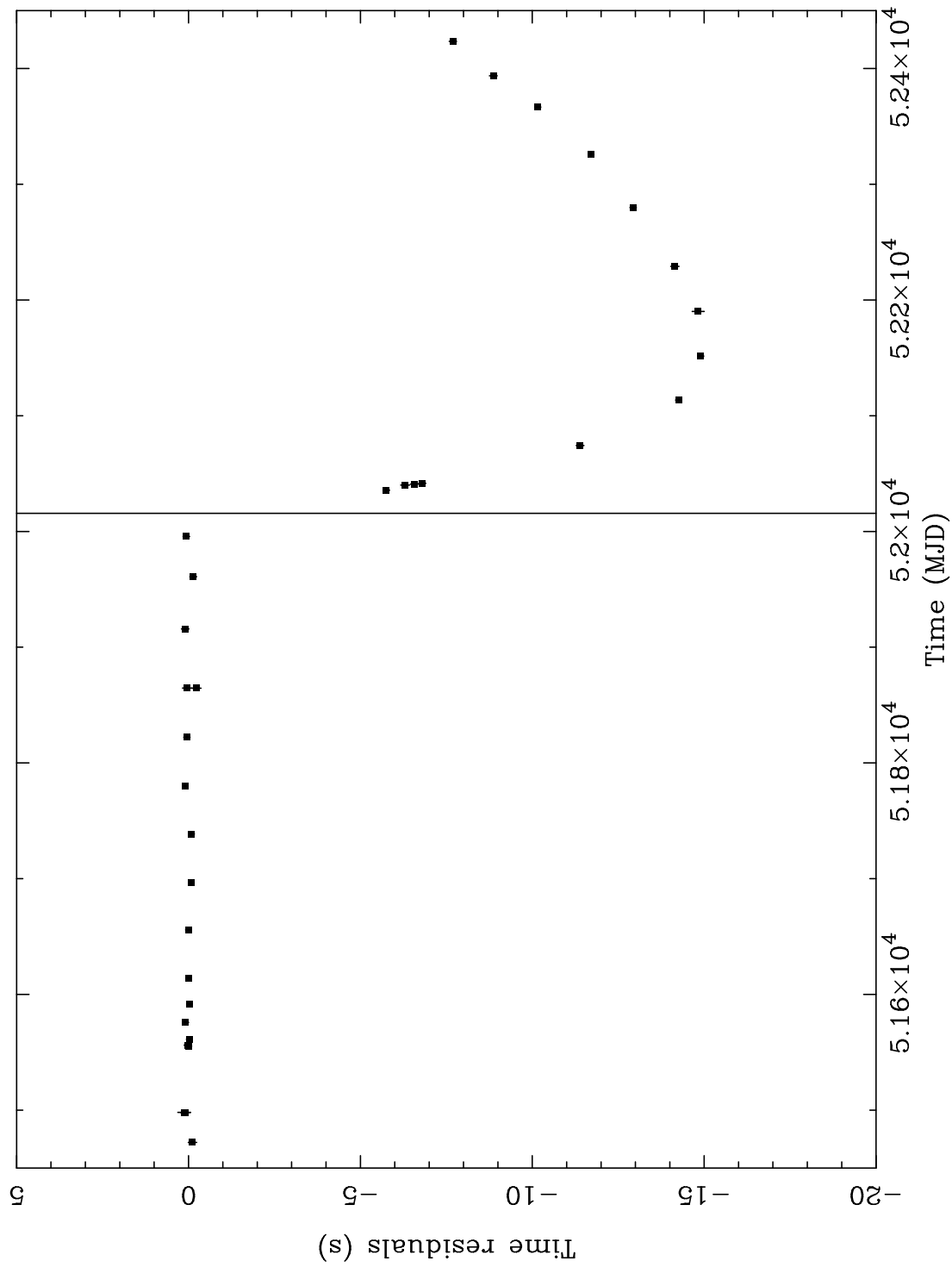


Fig. 2.—

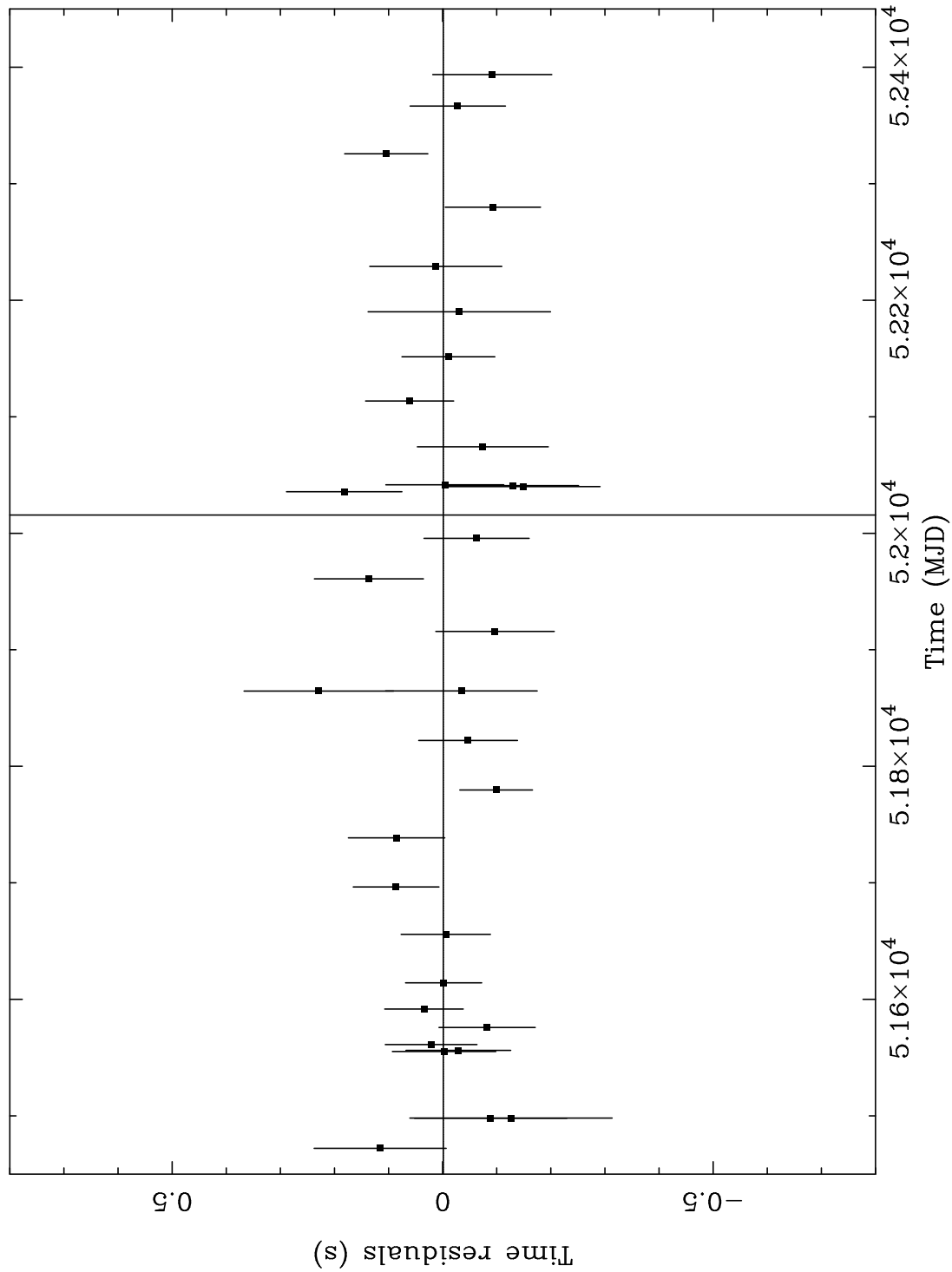


Fig. 3.—

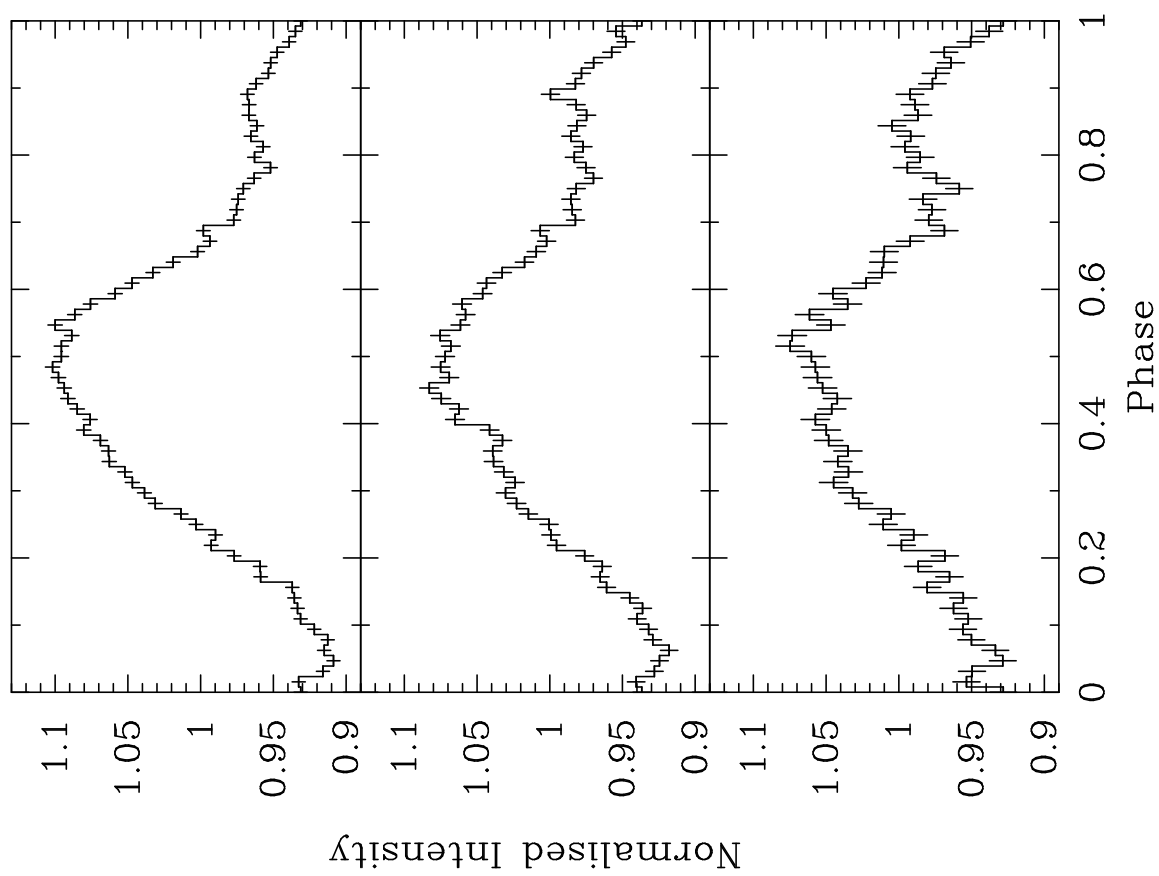


Fig. 4.—

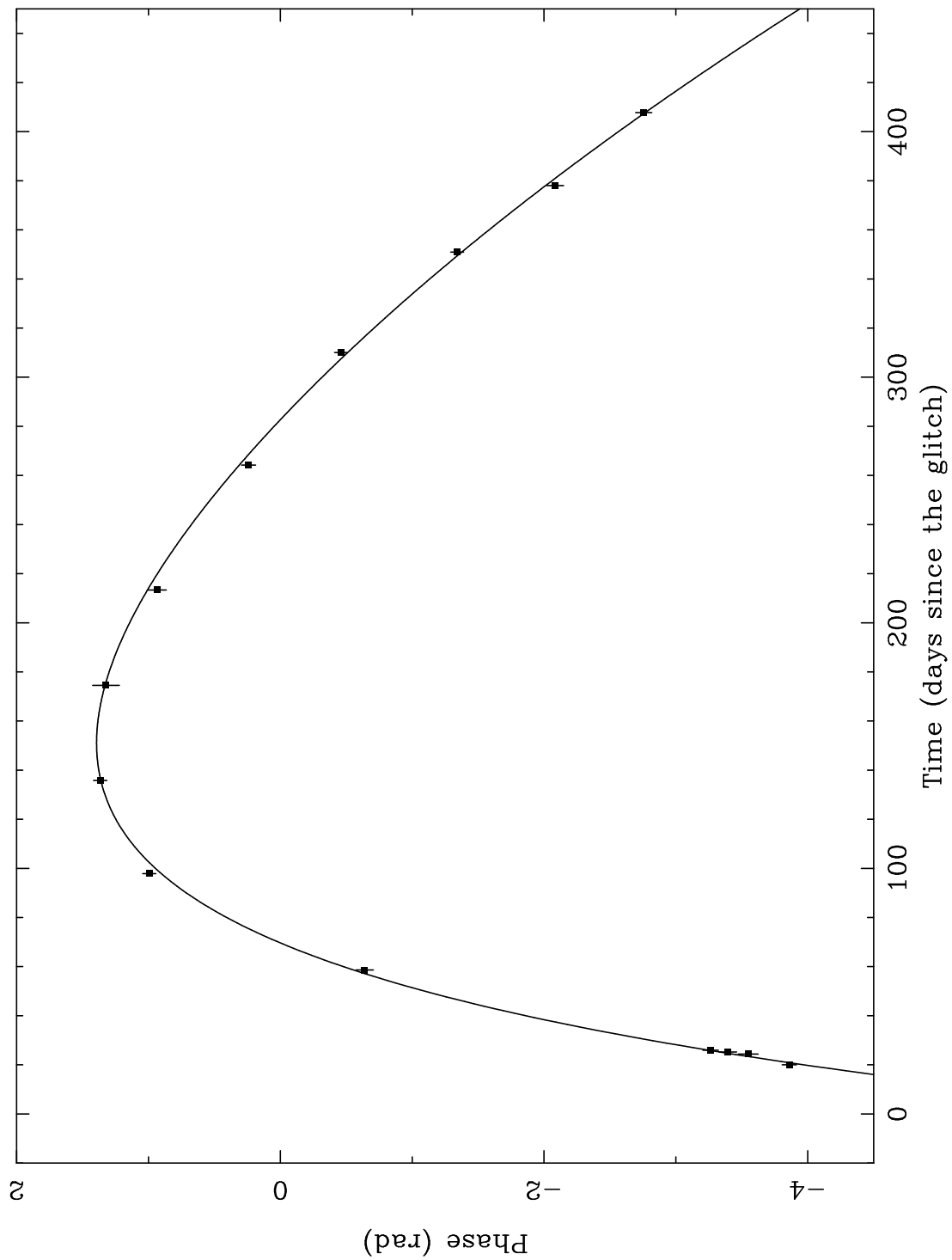


Fig. 5.—

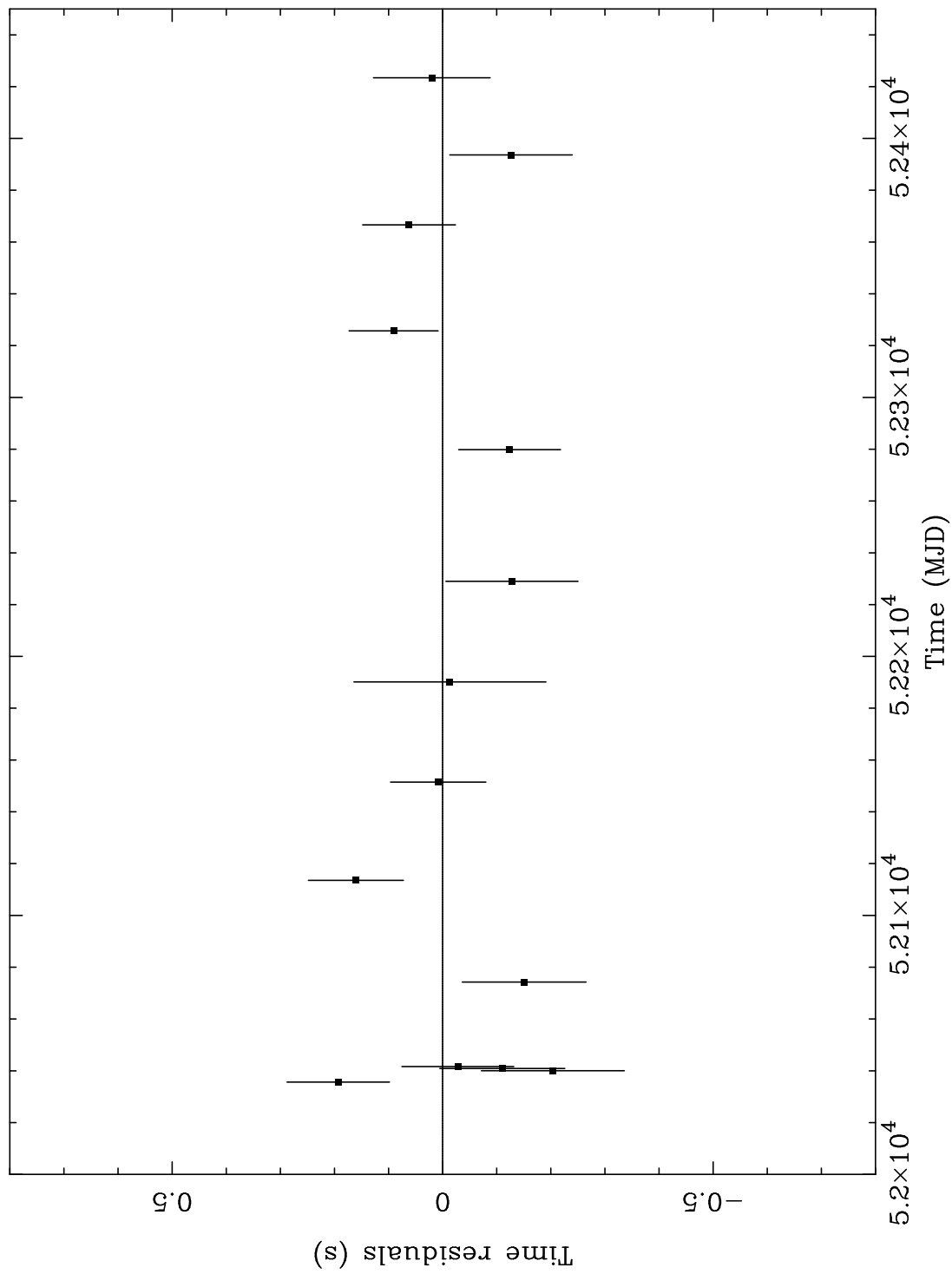


Fig. 6.—

Table 1: Measured rotational parameters of 1RXS J170849.0–400910 previous and after glitch N.1 and inferred glitch parameters.  $1\sigma$  errors in the last digit are quoted in parenthesis.

Spin Parameter	Pre–glitch N.1	Post–glitch N.1
Assumed		
glitch epoch (MJD)	51459.0	51459.0
$\nu$ (Hz)	0.0909136405(1)	.090913699(2)
$\dot{\nu} \times 10^{-13} s^{-1}$	-1.56809(12)	-1.595(2)
$\ddot{\nu}^a \times 10^{-23} s^{-3}$	-	4.9(6)
MJD range	50825–51446	51472–51995
N. of fitted points	39	19
r.m.s. (s)	0.16	0.09
$\frac{\Delta\nu}{\nu} \times 10^{-7}$	6.43(5)	
$\frac{\Delta\dot{\nu}}{\dot{\nu}} \times 10^{-2}$	1.72(5)	

<sup>a</sup>This parameter was found to be statistically non significant at the 99 % level in the fit to observed phases previous to glitch N.1. The corresponding values of  $\nu$  and  $\dot{\nu}$  are those derived by the best–fit model to the observed phases with  $\ddot{\nu}$  fixed at zero.

Table 2: Measured spin parameters and inferred glitch parameters for glitch N.2.  $1\sigma$  errors in the last digit are quoted in parenthesis

Spin Parameter	Pre-glitch N.2	Post-glitch N.2
Ref. Epoch(MJD)	51555.733	52041.254
$\nu$ (Hz)	0.0909123674(6)	0.090905939(5)
$\dot{\nu}$ ( $\times 10^{-13} s^{-2}$ )	-1.591(1)	-1.964(26)
$\ddot{\nu}$ ( $\times 10^{-23} s^{-3}$ )	4.9(6)	527(65)
$\nu^{(3)}$ ( $\times 10^{-28} s^{-4}$ )	-	-4.8(9)
$\nu^{(4)}$ $\times 10^{-35} s^{-5}$	-	2.1(5)
MJD range	51472–51995	52035–52423
N. of fitted points	19	14
<hr/>		
Polynomial Model		
<hr/>		
Assumed		
glitch epoch (MJD)	52015.65	52015.65
$\nu$ (Hz)	0.090906084(14)	0.090906387(13)
$\dot{\nu}$ ( $\times 10^{-13} s^{-2}$ )	-1.571(6)	-2.09(4)
$\ddot{\nu}$ ( $\times 10^{-23} s^{-3}$ )	4.9(6)	638(85)
$\nu^{(3)}$ ( $\times 10^{-28} s^{-4}$ )	-	-4.8(10)
$\nu^{(4)}$ $\times 10^{-35} s^{-5}$	-	2.1(5)
r.m.s. (s)	0.09	0.09
$\Delta\nu/\nu$ ( $\times 10^{-7}$ )		33(2)
$\Delta\dot{\nu}/\dot{\nu}$ ( $\times 10^{-2}$ )		33(3)
<hr/>		
Exponential Model		
<hr/>		
Assumed		
glitch epoch (MJD)		52015.65
$\delta\nu_{exp}$ ( $\times 10^{-9}$ Hz)		357(13)
$\tau$ (days)		50(2)
$\Delta\nu_l^a$ ( $\times 10^{-8} s^{-1}$ )		(-4.1 $\div$ 1.5)
$\Delta\dot{\nu}_l^b$ ( $\times 10^{-15} s^{-1}$ )		-1.382(27)
r.m.s. (s)		0.12

<sup>a</sup>This parameter was statistically non significant at the 99% confidence level in the fits and was then set equal to zero. A 99.9% confidence interval is reported in parenthesis

<sup>b</sup>The value and uncertainty of this parameter are determined with the non significant term  $\Delta\nu_l$  fixed at zero.

Table 3: Best-fit parameters of the average pulse profiles, obtained after folding the observations in the following three intervals: 1) 12 January 1998 (MJD 50825) – 25 September 1999 (MJD 51446); 2) 21 October 1999 (MJD 51472) – 2000 June 19 (MJD 51822); 3) 6 May 2001 (MJD 52035) – 2001 30 August (MJD 52151).  $1\sigma$  errors in the last digit are quoted in parenthesis

Parameter	Interval 1	Interval 2	Interval 3
N. of observations	39	11	7
$A_1(\times 10^{-2})$	8.09(8)	6.1(1)	5.1(2)
$A_2/A_1$	0.28(1)	0.29(2)	0.32(3)
$A_3/A_1$	0.15(1)	0.22(2)	0.26(3)
$A_4/A_1$	–	–	0.15(3)
$\psi_1$	0.229(2)	0.246(3)	0.230(5)
$(\psi_2 - \psi_1) \times 10^{-2}$	7.5(3)	4.3(6)	4(1)
$\psi_3 - \psi_1$	0.250(4)	0.227(5)	0.228(9)
$\psi_4 - \psi_1$	–	–	0.30(1)